Characterization of electrical noise limits in ultra-stable laser systems

J. Zhang, X. H. Shi, X. Y. Zeng, X. L. Lü, K. Deng, and Z. H. Lu

Citation: Review of Scientific Instruments **87**, 123105 (2016); doi: 10.1063/1.4971852
View online: https://doi.org/10.1063/1.4971852
View Table of Contents: http://aip.scitation.org/toc/rsi/87/12
Published by the American Institute of Physics

Characterization of electrical noise limits in ultra-stable laser systems

J. Zhang, X. H. Shi, X. Y. Zeng, X. L. Lü, K. Deng, and Z. H. Lu[a)]
MOE Key Laboratory of Fundamental Physical Quantities Measurement, School of Physics, Huazhong University of Science and Technology, Wuhan 430074, China

(Received 16 August 2016; accepted 25 November 2016; published online 16 December 2016)

We demonstrate thermal noise limited and shot noise limited performance of ultra-stable diode laser systems. The measured heterodyne beat linewidth between such two independent diode lasers reaches 0.74 Hz. The frequency instability of one single laser approaches 1.0×10^{-15} for averaging time between 0.3 s and 10 s, which is close to the thermal noise limit of the reference cavity. Taking advantage of these two ultra-stable laser systems, we systematically investigate the ultimate electrical noise contributions, and derive expressions for the closed-loop spectral density of laser frequency noise. The measured power spectral density of the beat frequency is compared with the theoretically calculated closed-loop spectral density of the laser frequency noise, and they agree very well. It illustrates the power and generality of the derived closed-loop spectral density formula of the laser frequency noise. Our result demonstrates that a 10^{-17} level locking in a wide frequency range is feasible with careful design. *Published by AIP Publishing.* [http://dx.doi.org/10.1063/1.4971852]

I. INTRODUCTION

Ultra-stable lasers are widely used in high resolution laser spectroscopy,[1] gravitational wave detection,[2] fundamental physics test,[3] and optical clocks.[4,5] To achieve very small frequency instability, the laser is typically servo locked to a high-finesse reference cavity using the Pound-Drever-Hall (PDH) technique.[6] The fundamental stability limitation of the reference cavity comes from the Brownian motions of the reference cavity materials.[7,8] With cavity length in the 7–20 cm range, typical thermal noise limit is about 3×10^{-16} to 1×10^{-15}.[9–20]

More information can be gained by looking at the spectral content of the laser frequency noise. Better understanding of the frequency noise can pave the way for laser stabilities approaching 10^{-17} levels. In the low Fourier frequency domain of less than 10-100 Hz, the thermal noise is the dominant noise source, and the thermal noise can be reduced by using longer reference cavities,[21–24] cavities with low loss angle crystalline coatings,[25] or cryogenic cavities made from single-crystal materials with a large mechanical Q factor.[26–28] In addition, intense research on the vibration effect, temperature effect, and residual amplitude modulation (RAM) effect give unambiguous instructions on how to build spectrally pure laser systems. For instance, vibration immune cavity design based on finite element analysis (FEA) can greatly reduce the cavity length change due to ground vibration.[10,11,15,29] The reference cavities are housed in vacuum chambers with large thermal time constants to suppress the temperature fluctuation effect on the cavity length.[13,14,16,30,31] In addition, cavity temperatures are maintained at their thermal expansion zero crossing points.

Less information is available for suppressing laser frequency noises in the high Fourier frequency domain.[32–35] Through down-conversion process, high frequency noise can affect the performance of optical clocks through Dick effect.[36] In the frequency range above 100 Hz, the main laser frequency noise contributions are laser free running noise due to limited servo bandwidth, photon shot noise, and electrical noise. Due to their large selection of wavelength range, low cost, small footprint, diode lasers have become very versatile tools in many precision measurement applications.[19] But diode lasers have much larger free running noise in the high frequency range compared with fiber lasers or solid-state lasers. As a consequence, it is well worth the effort to study the suppression of high frequency laser noise.

Previously, Day *et al.* derived an expression of the slope for the PDH frequency discriminator in the case of a quiet Nd:YAG solid state laser.[33] In this paper, we investigate the shot noise limited locking performance using a modified expression, taking into account the large servo bandwidth required for diode lasers. The magnitude of the slope for the PDH frequency discriminator is modelled without any free parameters. We directly measure all the parameters used in the expression. With all these efforts, we deduce the ultimate limit of the closed-loop spectral density of laser frequency noise. The theoretical analysis agrees well with the measured power spectral density of the beat note of two ultra-stable lasers.

In Sec. II, we describe the experimental setup of two independent 1070 nm ultra-stable diode laser systems to characterize frequency instability and noise contributions. Thermal noise limited performance is demonstrated. The Allan deviation of the beat note of the two ultra-stable diode lasers reaches a level of 1×10^{-15} at 0.3 s–10 s, which is close to the thermal noise limit of two 10 cm long ULE reference cavities. The stabilized diode laser is amplified and then frequency quadrupled to 267.4 nm to serve as a local oscillator for an $^{27}Al^{+}$ optical frequency standard. In Sec. III, we perform theoretical calculations on the closed-loop frequency spectral density of frequency noise in a stabilized laser system. In addition, we determine the minimum frequency noise spectral density in a real laser system. In Sec. IV, we measure the

a)Electronic mail: zehuanglu@mail.hust.edu.cn

parameters used in the expression, taking advantage of the two thermal noise limited ultra-stable laser systems. We analyze the measured linear frequency power spectral density of frequency noise for the beat note as the out-loop signal, and find that not only laser power injected to the cavity but also cavity linewidth and cavity coupling efficiency play critical roles in the electrical noise level. We conclude in Sec. V.

II. EXPERIMENTAL SETUP

The two ultra-stable reference cavities (ATFilms, ATF-6020-2) that we used are entirely made of ULE glass. Each horizontally mounted cavity is 10 cm long, and its diameter is 7 cm with a 0.5 in.-diameter bore hole along the central axis. Two 1 in.-diameter ULE mirrors are optically contacted to both sides of the spacer. The thermal noise limit of each reference cavity is estimated to be 7.7×10^{-16}, dominated by the Brownian motion of the ULE mirror substrates.[7,8] We named these two reference cavities as Cav1 and Cav2, respectively. Their TEM_{00} mode linewidths are measured to be 13.6 kHz and 4.5 kHz, corresponding to finesses of 110 000 and 333 000, respectively. The reference cavities are housed in two vacuum chambers with pressures less than 1×10^{-6} Pa for isolation from air pressure fluctuations, temperature fluctuations, and acoustic noise. The temperature of vacuum chambers is stabilized by digital temperature control loops to T_0(Cav1) = 36.8 °C and T_0(Cav2) = 36.3 °C, respectively. These temperatures are measured to be the zero crossing temperatures of the coefficient of thermal expansion for the cavities.[31] The temperature fluctuation is about 1 mK in 24 h. The temperature stabilized vacuum chambers house two polished gold-coated copper shields, which provide additional passive isolation of external temperature fluctuations. The ULE cavities are placed on four viton bars on the notched surfaces where the mounting positions are optimized to minimize the sensitivity to vibration through FEA. In addition, the two vacuum chambers are separately placed on two active vibration isolation (AVI) stages.

Figure 1 shows the optical setup of the two ultra-stable laser systems. The laser source is a Littrow-Hänsch-type grating stabilized external cavity diode laser (Toptica, DL pro) operating at around 1070 nm, which is four times the ultraviolet wavelength of the clock transition in an aluminum ion. It has a free running fast linewidth of ~100 kHz and the output power is about 50 mW after a 70 dB isolator and a fiber coupler with a 30 cm-long polarization maintaining fiber. They are used to prevent spectral disturbances caused by optical feedback and to provide a clean laser mode, respectively. The diode laser is locked to the TEM_{00} mode of the reference cavity with the PDH method. The laser beam is sent through a Glan-Taylor polarizer with an extinction ratio of 10^6:1 to improve the polarization purity, which can greatly suppress laser power fluctuation due to the residual light polarization ellipticity. Two laser frequencies are phase modulated by a 21 MHz electro-optic modulator (EOM) and a 28 MHz EOM, respectively. We deliberately choose two different modulation frequencies to avoid error signal disturbance within the locking bandwidth. The modulation indices for the two EOMs are tuned to an

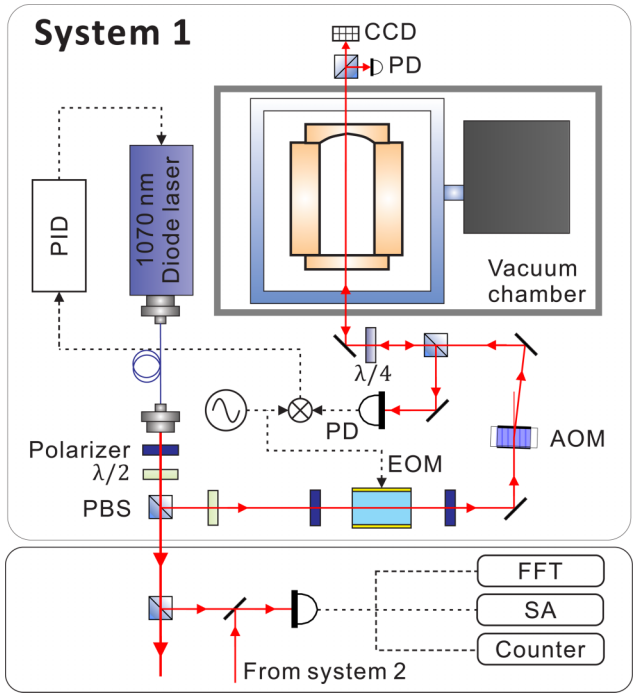

FIG. 1. Experimental setup of the ultra-stable laser system. The red solid line shows the optical path and the black dashed line represents the electronic path.

optimal value of 1.08 to maximize the slope of the PDH error signal. To reduce the RAM effect of the EOMs, Glan-Taylor polarizers are placed in front of the EOMs to get high polarization purity along the modulation axis of the EOMs. Furthermore, the EOMs are actively temperature stabilized with a temperature fluctuation less than 10 mK. Each laser beam is focused on the flat coupling mirror of the reference cavity with a diameter of 520 μm in order to mode match to the TEM_{00} mode and typical coupling efficiencies for Cav1 and Cav2 are ~30% and ~60%, respectively. We normally send 10–20 μW of laser power to the reference cavity for the PDH lock. The reflected signal is detected with an InGaAs PIN photodiode. The total optical path length is about 1.5 m.

The detected signal is demodulated using a frequency mixer (Mini Circuits, ZP-3+). The same radio-frequency (RF) signal for EOM driving is used as the local oscillator (LO) input. In order to obtain the correct sine term at the modulation frequency of the error signal, we shift the phase of the RF signal with a delay box (Ortec, 425A). The obtained error signal is sent through a fast analog linewidth controller (Toptica, FALC) that acts as a low pass filter. The output is split into two parts. One is used for fast feedback control of the driving current of the diode laser with a measured ~2 MHz servo bandwidth. The other one is used for slow feedback control of the cavity length of the diode laser with a measured 2 kHz servo bandwidth. The slow control is achieved by applying the feedback signal to a piezo that is glued to the grating inside the diode laser cavity.

After thoroughly characterizing the effect of temperature fluctuation, vibration, power fluctuation, and residual amplitude modulation effect, we measure the beat frequency of the two locked diode lasers to evaluate the performance of the

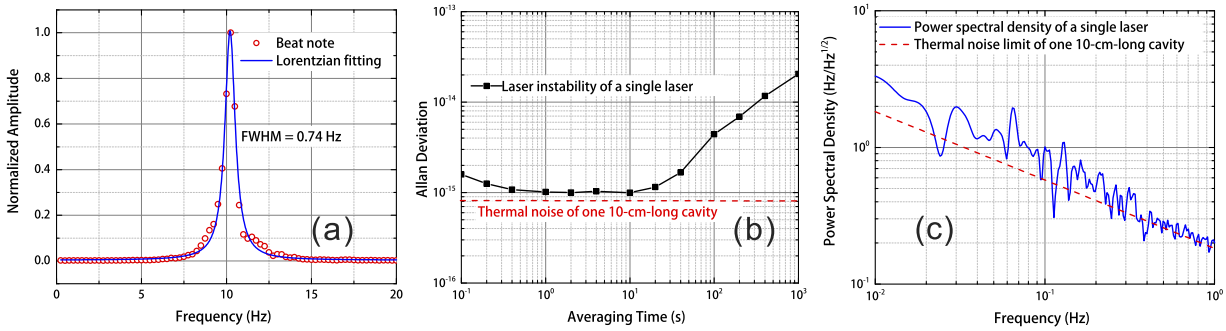

FIG. 2. Results of the ultrastable laser performance. (a) Optical beat note signal representing the short-term linewidth of the two lasers stabilized to Cav1 and Cav2 cavities. The red circles show an average of twenty recorded beat notes, the FWHM is fitted to be 0.74 Hz using a Lorentzian function. (b) Fractional frequency instability of a single laser, assuming two identical systems. The fractional frequency instability for a single laser is about 1.0×10^{-15} from 0.3 s to 10 s, shown with the black square points. (c) The blue curve is the power spectral density of a single laser, while the red dashed line is the thermal noise limit of the 10-cm-long cavity.

stabilized lasers. Figure 2(a) shows a down converted beat note frequency measured with a fast-Fourier-transform (FFT) spectrum analyzer (Stanford Research Systems, SR785). A resolution bandwidth of 0.25 Hz is used. The red circles are the measured beat frequency which are averaged 20 times, and the blue curve is a Lorentzian fit. The full width at half maximum (FWHM) of the beat signal is 0.74 Hz. Assuming two identical laser systems, the linewidth of one single laser is 0.52 Hz. In addition, we down-convert the beat frequency to around 1 MHz, and record the frequency with a frequency counter (Agilent, 53230A) with a 0.1 s gate time. All measurement instruments including the spectrum analyzer, the counter, and the signal generators are all referenced to an active hydrogen maser (Symmetricom, MHM2010). As shown in Fig. 2(b), the fractional frequency instability for a single laser is around 1.0×10^{-15} from 0.3 s to 10 s, which is close to the thermal noise limit of the reference cavities. The power spectral density of a single laser is shown in Fig. 2(c) with a blue curve, while the red dashed line is the thermal noise limit of the 10-cm-long cavity.

Based on these two laser systems with thermal noise limited performance, we characterize the electrical noise contributions to the achievable frequency instability of the diode lasers in Secs. III and IV. With better understanding of the electrical noise level, it will greatly help the development of the next generation ultra-stable lasers aiming at the 10^{-17} level.

III. DERIVATION OF LASER FREQUENCY NOISE EXPRESSION

Laser frequency stabilization discussed in Sec. II can be modeled using control theory.[33] The schematic representation of a general laser frequency stabilization process is shown in Fig. 3. An error signal is obtained when a diode laser frequency is gone through a frequency discriminator with a slope of $D_\nu(f)$ to convert optical frequency fluctuations into electrical signal fluctuations. The frequency discriminator noise is represented by S_{disc}. The error signal is corrected by a servo to generate enough gain and phase margin. The servo has a frequency dependent gain coefficient $G(f)$, and the servo noise is represented by $S_{servo}(f)$. The corrected error signal is fed back to the laser actuator with a coefficient of K which pulls the laser frequency back to the cavity's transmission peak. The actuator noise and the diode laser free running noise are represented by $S_{actuator}(f)$ and $S_{laser}(f)$, respectively. These two noises cannot be distinguished, and are added onto the diode laser in a single step.

The closed-loop linear spectral density of frequency noise, S_{cl}, is given by

$$S_{cl} = \sqrt{\left|\frac{S_{laser} + S_{actuator}}{1 + KGD_\nu}\right|^2 + \left|\frac{KS_{servo}}{1 + KGD_\nu}\right|^2 + \left|\frac{KGS_{disc}}{1 + KGD_\nu}\right|^2}, \quad (1)$$

where D_ν is frequency discriminator slope in units of V/Hz, G is the frequency dependent servo gain in unit of V/V, and K is the actuator coefficient in units of Hz/V. The closed-loop frequency noise can be separated as three parts: free running laser noise, servo noise, and discriminator noise. Free running laser noise and servo noise can be greatly suppressed with a very large actuator coefficient K and servo gain G. In the limit of large K and G, the closed-loop spectral density of laser frequency noise, $S_{cl,\text{limit}}$, can be expressed as

$$S_{cl,\text{limit}} = \frac{S_{disc}}{|D_\nu|}. \quad (2)$$

It is clear that $S_{cl,\text{limit}}$ is determined by the noise spectral density of the frequency discriminator and the discriminator slope.

For the PDH technique, frequency modulation is used to detect the laser frequency noise in higher Fourier frequency

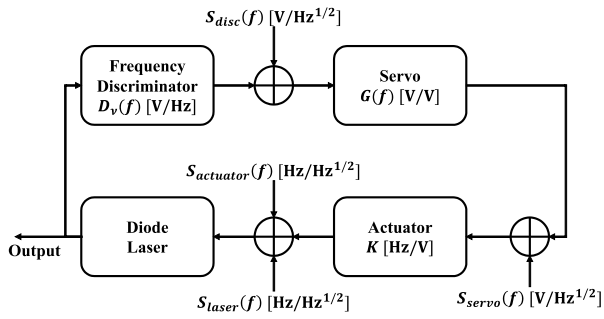

FIG. 3. Schematic representation of laser frequency stabilization to a reference cavity with the PDH technique.

in order to minimize the technical noise contribution, such as intensity noise. The S_{disc} is the output of the frequency mixer in the PDH error signal detection, which can be written as

$$S_{disc} = \kappa S_{RF} = \kappa R\sqrt{\mathrm{NEP}^2 + 2h\nu P_{det}/\eta_d}, \tag{3}$$

where κ is the conversion loss of the frequency mixer with a saturated LO power, S_{RF} is the noise power spectral density in the RF port of the mixer, R is the responsivity of the combined system of the PD and the transimpedance amplifier in units of V/W, NEP is the optical noise equivalent power of the PD for the PDH error signal detection, η_d is the quantum efficiency of the detector, and P_{det} is the laser power that is reflected back from the cavity and detected by the PD. P_{det} can be expressed as

$$P_{det} = (1-\alpha)J_0^2(\beta)P_{in} + 2J_1^2(\beta)P_{in}, \tag{4}$$

where α is the coupling efficiency of the optical reference cavity and P_{in} is the injected laser power to the optical reference cavity, and $J_0(\beta)$ and $J_1(\beta)$ are the zeroth order and the first order Bessel functions, respectively. We neglect higher order terms when $\beta = 1.08$. As can be seen, both laser shot noise and electrical noise from the PD contribute to the noise of the discriminator, especially when weak laser power is used. High laser power will heat the ultra-stable cavity's mirrors and coatings which degrades the frequency stability.

According to Eq. (2), a large value of the slope of the frequency discriminator is essential in the PDH laser frequency stabilization system. The slope of the frequency discriminator has a frequency dependence such that its value decreases when the laser frequency is away from the cavity transmission peak. The expression for this slope can be written as[33,34]

$$\begin{aligned} D_\nu(f) &= \frac{8J_0(\beta)J_1(\beta)RP_{in}}{\Delta\nu_c}\sqrt{\frac{\mathrm{sinc}^2(\pi f/F\Delta\nu_c)}{1+\frac{4F^2}{\pi^2}\sin^2(\pi f/F\Delta\nu_c)}} \\ &\approx \frac{8J_0(\beta)J_1(\beta)RP_{in}}{\Delta\nu_c}\frac{1}{1+2if/\Delta\nu_c}, \end{aligned} \tag{5}$$

where F is the finesse of the cavity, $\Delta\nu_c$ is the linewidth of the cavity, f is the frequency difference between the laser frequency and the cavity's transmission peak. Equation (5) is the voltage signal at the PD output end without considering the effect of the mixer demodulation process and the reference cavity's coupling efficiency. Taking that into account, Eq. (5) becomes

$$D_\nu(f) = \kappa\alpha\frac{8J_0(\beta)J_1(\beta)RP_{in}}{\Delta\nu_c}\frac{1}{1+2if/\Delta\nu_c}. \tag{6}$$

In this expression, the amplitude and the phase of the PDH discriminator slope demonstrate a low-pass filter function with Fourier frequency. The phase shift in the error signal and time delay in the control loop prevent us from reaching an unlimited servo bandwidth, therefore a proper servo is very important in this system.

Substituting Eqs. (3) and (6) into Eq. (2), we obtain the discriminator noise limit of the PDH locking in the dispersion mode

$$S_{cl,\mathrm{limit}} = \frac{\sqrt{\mathrm{NEP}^2 + 2h\nu P_{det}/\eta_d}}{8\alpha J_0(\beta)J_1(\beta)P_{in}}|\Delta\nu_c + 2if|. \tag{7}$$

The discriminator limit has a white frequency noise characteristic for low frequencies, and increases by 20 dB/decade when f is sufficiently larger than the linewidth of the cavity. To obtain a low discriminator noise limit and reach the shot noise limit, NEP of the PD should be as small as possible, enough laser power should be used until the laser intensity noise affects the final frequency stability, and α should be as large as possible.

Equation (7) has been experimentally proved to be valid, but the measurement process is too tedious. To simplify the system characterization process, we rewrite Eqs. (6) and (7) as

$$D_\nu(f) = \frac{D_0}{1+2if/\Delta\nu_c}, \tag{8}$$

$$S_{cl,\mathrm{limit}} = \frac{S_{disc}}{D_0}|1+2if/\Delta\nu_c|. \tag{9}$$

D_0 is the discriminator slope at $f = 0$ that can be measured in a real system. To determine the ultimate limit of the closed-loop laser frequency noise spectral density, we can directly measure the discriminator noise S_{disc}, D_0, and the linewidth of the cavity $\Delta\nu_c$.

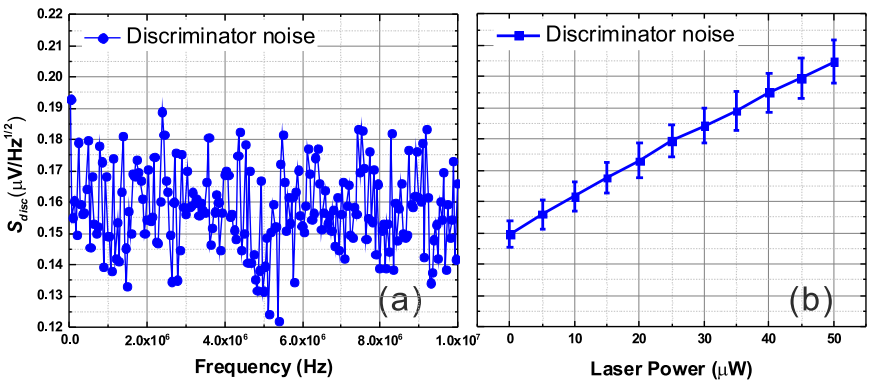

FIG. 4. (a) The blue circled points show the noise spectral density of the discriminator without laser input onto the PD, measured with the spectrum analyzer. (b) Discriminator noise vs. laser power detected by the PD.

IV. LASER FREQUENCY NOISE ANALYSIS

Taking advantage of the two developed 1070 nm ultra-stable diode laser systems, we can verify the ultimate limit of the closed-loop laser frequency noise spectral density using the beat note of the two laser systems. We measure all the needed parameters in the two systems, and make comparisons with the theory discussed in Sec. III.

First, we measure the discriminator noise S_{disc} from the IF port of the mixer. The measurement results are shown in Fig. 4. The noise spectral density of the discriminator without laser input onto the PD is shown in Fig. 4(a), measured with a spectrum analyzer (Agilent, N9030A). We also measure the changes of the discriminator noise with laser power detected by the PD, as shown in Fig. 4(b).

To find the value of the discriminator slope D_0, we cannot simply measure it by sweeping the laser frequency over the cavity resonance frequency since the free running diode laser's linewidth is more than one order of magnitude larger than that of the cavity. To solve this problem, we use the beat signal of the two stabilized diode laser systems. With system 2 as reference, we modulate the error signal of laser system 1 with a 0.2 Hz $V_{pp} = 4$ mV square wave while keeping the laser locked to the cavity. A square wave modulation with an amplitude of $f_{pp} = 1$ kHz is obtained from the beat frequency of the two lasers, as shown in Fig. 5. The measurement indicates that a small introduced voltage perturbation can cause a corresponding frequency change. Thus, $D_0 = V_{pp}/f_{pp} = 4$ μV/Hz for laser system 1 when the input laser power is 20 μW. In this way, the D_0 for different laser systems and different input powers can be measured. The discriminator slope of system 2 is measured to be 30 μV/Hz with a 20 μW input power. The difference between the two discriminator slopes is caused by different cavity linewidths and different laser coupling efficiencies into the cavities. The laser coupling efficiency of system 2 is about two times better than that of system 1.

By substituting all the measured parameters into Eq. (9), we can obtain the contribution of the two cavities' discriminator noises. We measure the frequency noise of the beat frequency of the two lasers with IQ demodulation using the RF spectrum analyzer.[37] The IQ method can distinguish phase noise and amplitude noise from the beatnote. The power spectral density of the beat frequency under different input powers is recorded and compared with the corresponding discriminator noises, as shown in Fig. 6. We fix the parameters of system 2 as $P_{in} = 20$ μW, $S_{disc} = 0.17$ μV/$\sqrt{\text{Hz}}$, and $D_0 = 30$ μV/Hz. And then we change the input power of system 1 from 10 μW to 44 μW. Figures 6(a) and 6(b) demonstrate that the power spectral density of the beat frequency is limited by the discriminator noise of system 1 from 1 kHz to 100 kHz, when the input power is 10 μW and 20 μW. For Fourier frequencies larger than 100 kHz, K, G, and D_ν are no longer much larger than 1, so the simplification of Eq. (9) does not work in these frequencies. When the laser power is 44 μW in system 1, we can see that the lowest power spectrum density reaches a level of 0.04 Hz/$\sqrt{\text{Hz}}$. This level is not limited by the electrical noises, demonstrating shot noise limited performance. Other noise sources, such as vibration noise, might also contribute to this noise level. But they must be in much smaller levels, otherwise in Fig. 6(b) the measured noise spectrum will not agree with the discriminator noise.

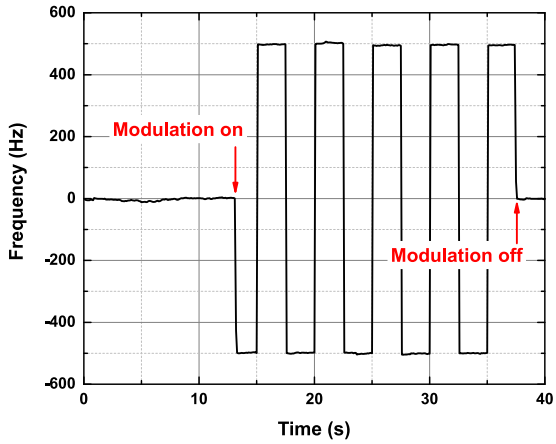

FIG. 5. Discriminator slope measured with the beat frequency of the two ultra-stable lasers, when the laser locked to Cav1 is modulated by a 0.2 Hz 4 mV peak to peak square wave. A 1 kHz peak to peak frequency modulation is observed.

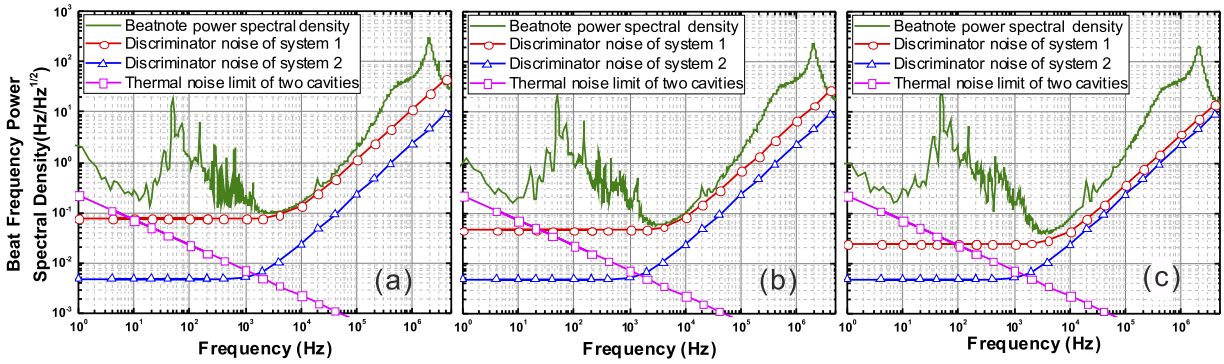

FIG. 6. Linear power spectral density of beat note frequency and corresponding discriminator noises of two systems under different input powers. We keep the parameters of system 2 constant with $P_{in} = 20$ μW, $S_{disc} = 0.17$ μV/$\sqrt{\text{Hz}}$, and $D_0 = 30$ μV/Hz. And then we change the input power of system 1 from 10 μW to 44 μW. (a) $P_{in} = 10$ μW, $S_{disc} = 0.15$ μV/$\sqrt{\text{Hz}}$, $D_0 = 2$ μV/Hz. The minimum value of the beatnote power spectral density is 0.08 Hz/$\sqrt{\text{Hz}}$, limited by the discriminator noise of system 1. (b) $P_{in} = 20$ μW, $S_{disc} = 0.17$ μV/$\sqrt{\text{Hz}}$, $D_0 = 4$ μV/Hz. The minimum value of the beatnote power spectral density is 0.06 Hz/$\sqrt{\text{Hz}}$, limited by the discriminator noise of system 1. (c) $P_{in} = 44$ μW, $S_{disc} = 0.21$ μV/$\sqrt{\text{Hz}}$, $D_0 = 8.7$ μV/Hz. The minimum value of the beatnote power spectral density is 0.04 Hz/$\sqrt{\text{Hz}}$. The thermal noise limit is also indicated with an open squared line.

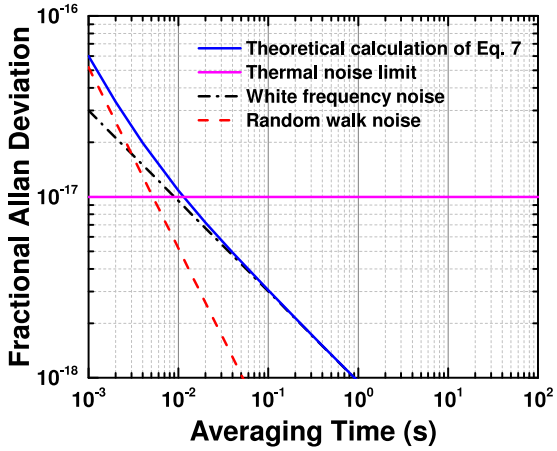

FIG. 7. Fractional frequency instability calculated from Eq. (7), with $\delta\nu_c = 4.5$ kHz, $P_{in} = 50$ μW, and $\alpha = 0.5$. The electrical noise contribution can be suppressed down to the level of 10^{-17} at averaging time larger than 0.01 s. The black dashed curve shows the white frequency noise contribution, and the red dashed curve shows the random walk noise contribution.

The peaks in the low frequency range are caused by power line noise at 50 Hz and its harmonic frequency. There are also some peaks caused by vibrational noise.

The development speed of ultra-stable lasers is fascinating, and the laser stability is approaching a level of 10^{-17}.[24] Great care has to be paid to suppress the electrical noise down to the level of 10^{-17}. Taking Eq. (7) as an ideal case, we can obtain the ultimate limit of the spectral noise density and calculate the corresponding fractional frequency instability. For example, in Fig. 7, according to Eq. (7), we can calculate $S_{cl,limit} = 3.77 \times 10^{-4}|1 + \frac{2if}{\Delta\nu_c}|\,\mathrm{Hz}/\sqrt{\mathrm{Hz}}$, using a 4.5 kHz linewidth reference cavity, 50 μW input power, and $\alpha = 0.5$. We then convert the power spectral density of the laser frequency noise into Allan deviation. From the slopes of power spectral density, we know that the types of noise are white frequency noise and random walk noise.[38] As shown in Fig. 7, the ultimate limit contribution of the electrical noise is estimated to be in the level of 10^{-17} in a wide frequency range.

V. CONCLUSION

In conclusion, we demonstrate thermal noise limited and shot noise limited performance of ultra-stable diode laser systems. The fractional frequency instability of a single diode laser is around 1.0×10^{-15} between 0.3 s and 10 s averaging time, which is close to the thermal noise limit of the reference cavity. The FWHM of the optical beat signal is 0.74 Hz, indicating a 0.52 Hz linewidth of one single laser. Taking advantage of the two ultra-stable laser systems, we investigate the ultimate limit of the electrical noise contributions and derive expressions for the closed-loop laser frequency noise spectral density. The measurements of the relevant parameters based on the two laser systems are discussed as well, including discriminator noise at the mixer end, and real discriminator slope. In addition, we compare the experimental power spectral density of the beat note frequency with the theoretical calculated closed-loop laser frequency noise spectral density, and the results agree very well. So we can realistically estimate the electrical noise contribution to the system performance, and offer guidelines in designing an ultra-stable laser system that has stability approaching 10^{-17} level in the future.

ACKNOWLEDGMENTS

The project is partially supported by the National Basic Research Program of China (Grant No. 2012CB821300), the National Natural Science Foundation of China (Grant Nos. 91336213, 91536116, and 11174095), and Program for New Century Excellent Talents by the Ministry of Education (No. NCET-11-0176).

[1]W. H. Oskay, W. M. Itano, and J. C. Bergquist, "Measurement of the $^{199}Hg^+$ $5d^96s^2\ ^2D_{5/2}$ electric quadrupole moment and a constraint on the quadrupole shift," Phys. Rev. Lett. **94**, 163001 (2005).
[2]B. Willke, K. Danzmann, M. Frede, P. King, D. Kracht, P. Kwee, O. Puncken, R. L. Savage, B. Schulz, F. Seifert, C. Veltkamp, S. Wagner, P. Weβels, and L. Winkelmann, "Stabilized lasers for advanced gravitational wave detectors," Classical Quantum Gravity **25**, 114040 (2008).
[3]M. Nagel and A. Peters, "Towards an ultra-stable optical sapphire cavity system for testing Lorentz invariance," e-print arXiv:1112.3623v1 (2011).
[4]T. Rosenband, D. B. Hume, P. O. Schmidt, C. W. Chou, A. Brusch, L. Lorini, W. H. Oskay, R. E. Drullinger, T. M. Fortier, J. E. Stalnaker, S. A. Diddams, W. C. Swann, N. R. Newbury, W. M. Itano, D. J. Wineland, and J. C. Bergquist, "Frequency ratio of Al^+ and Hg^+ single-ion optical clocks; metrology at the 17th decimal place," Science **319**, 1808–1812 (2008).
[5]A. D. Ludlow, M. M. Boyd, J. Ye, E. Peik, and P. O. Schmidt, "Optical atomic clocks," Rev. Mod. Phys. **87**, 637 (2015).
[6]R. W. P. Drever, J. L. Hall, F. V. Kowalski, J. Hough, G. M. Ford, A. J. Munley, and H. Ward, "Laser phase and frequency stabilization using an optical resonator," Appl. Phys. B **31**, 97–105 (1983).
[7]K. Numata, A. Kemery, and J. Camp, "Thermal-noise limit in the frequency stabilization of lasers with rigid cavities," Phys. Rev. Lett. **93**, 250602 (2004).
[8]T. Kessler, T. Legero, and U. Sterr, "Thermal noise in optical cavities revisited," J. Opt. Soc. Am. B **29**, 178–184 (2012).
[9]B. C. Young, F. C. Cruz, W. M. Itano, and J. C. Bergquist, "Visible lasers with subhertz linewidths," Phys. Rev. Lett. **82**, 3799–3802 (1999).
[10]T. Nazarova, F. Riehle, and U. Sterr, "Vibration-insensitive reference cavity for an ultra-narrow-linewidth laser," Appl. Phys. B **83**, 531 (2006).
[11]S. A. Webster, M. Oxborrow, and P. Gill, "Vibration insensitive optical cavity," Phys. Rev. A **75**, 011801(R) (2007).
[12]A. D. Ludlow, X. Huang, M. Notcutt, T. Zanon-Willette, S. M. Foreman, M. M. Boyd, S. Blatt, and J. Ye, "Compact, thermal-noise-limited optical cavity for diode laser stabilization at 1×10^{-15}," Opt. Lett. **32**, 641–643 (2007).
[13]J. Alnis, A. Matveev, N. Kolachevsky, Th. Udem, and T. W. Hänsch, "Subhertz linewidth diode lasers by stabilization to vibrationally and thermally compensated ultralow-expansion glass Fabry-Pérot cavities," Phys. Rev. A **77**, 053809 (2008).
[14]S. A. Webster, M. Oxborrow, S. Pugla, J. Millo, and P. Gill, "Thermal-noise-limited optical cavity," Phys. Rev. A **77**, 033847 (2008).
[15]J. Millo, D. V. Magalhães, C. Mandache, Y. Le Coq, E. M. L. English, P. G. Westergaard, J. Lodewyck, S. Bize, P. Lemonde, and G. Santarelli, "Ultrastable lasers based on vibration insensitive cavities," Phys. Rev. A **79**, 053829 (2009).
[16]P. Dubé, A. A. Madej, J. E. Bernard, L. Marmet, and A. D. Shiner, "A narrow linewidth and frequency-stable probe laser source for the $^{88}Sr^+$ single ion optical frequency standard," Appl. Phys. B **95**, 43–54 (2009).
[17]Y. N. Zhao, J. Zhang, A. Stejskal, T. Liu, V. Elman, Z. H. Lu, and L. J. Wang, "A vibration-insensitive optical cavity and absolute determination of its ultrahigh stability," Opt. Express **17**, 8970 (2009).
[18]S. T. Dawkins, R. Chicireanu, M. Petersen, J. Millo, D. V. Magalhães, C. Mandache, Y. Le Coq, and S. Bize, "An ultra-stable referenced interrogation system in the deep ultraviolet for a mercury optical lattice clock," Appl. Phys. B **99**, 41-46 (2010).
[19]Y. N. Zhao, J. Zhang, J. Stuhler, G. Schuricht, F. Lison, Z. H. Lu, and L. J. Wang, "Sub-hertz frequency stabilization of a commercial diode laser," Opt. Commun. **283**, 4696 (2010).

[20]H. Q. Chen, Y. Y. Jiang, S. Fang, Z. Y. Bi, and L. S. Ma, "Frequency stabilization of Nd:YAG lasers with a most probable linewidth of 0.6 Hz," J. Opt. Soc. Am. B **30**, 1546 (2013).
[21]Y. Y. Jiang, A. D. Ludlow, N. D. Lemke, R. W. Fox, J. A. Sherman, L.-S. Ma, and C. W. Oates, "Making optical atomic clocks more stable with 10^{-16} level laser stabilization," Nat. Photonics **5**, 158 (2011).
[22]S. Amairi, T. Legero, T. Kessler, U. Sterr, J. B. Wübbena, O. Mandel, and P. O. Schmidt, "Reducing the effect of thermal noise in optical cavities," Appl. Phys. B **113**, 233–242 (2013).
[23]J. Keller, S. Ignatovich, S. A. Webster, and T. E. Mehlstäubler, "Simple vibration-insensitive cavity for laser stabilization at the 10^{-16} level," Appl. Phys. B **116**, 203-210 (2014).
[24]S. Häfner, S. Falke, C. Grebing, S. Vogt, T. Legero, M. Merimaa, C. Lisdat, and U. Sterr, "8×10^{-17} fractional laser frequency instability with a long room-temperature cavity," Opt. Lett. **40**, 2112 (2015).
[25]G. D. Cole, W. Zhang, M. J. Martin, J. Ye, and M. Aspelmeyer, "Tenfold reduction of Brownian noise in high-reflectivity optical coatings," Nat. Photonics **7**, 644 (2013).
[26]T. Kessler, C. Hagemann, C. Grebing, T. Legero, U. Sterr, F. Riehle, M. J. Martin, L. Chen, and J. Ye, "A sub-40-mHz-linewidth laser based on a silicon single-crystal optical cavity," Nat. Photonics **6**, 687 (2012).
[27]C. Hagemann, C. Grebing, C. Lisdat, S. Falke, T. Legero, U. Sterr, F. Riehle, M. J. Martin, and J. Ye, "Ultrastable laser with average fractional frequency drift rate below 5×10^{-19}/s," Opt. Lett. **39**, 5102 (2014).
[28]E. Wiens, Q. F. Chen, I. Ernsting, H. Luckmann, U. Rosowski, A. Nevsky, and S. Schiller, "Silicon single-crystal cryogenic optical resonator," Opt. Lett. **39**, 3242 (2014).
[29]L. S. Chen, J. L. Hall, J. Ye, T. Yang, E. J. Zang, and T. C. Li, "Vibration-induced elastic deformation of Fabry-Perot cavities," Phys. Rev. A **74**, 053801 (2006).
[30]J. Zhang, Y. X. Luo, B. Ouyang, K. Deng, Z. H. Lu, and J. Luo, "Design of an optical reference cavity with low thermal noise limit and flexible thermal expansion properties," Eur. Phys. J. D **67**, 46 (2013).
[31]J. Zhang, W. Wu, X. H. Shi, X. Y. Zeng, K. Deng, and Z. H. Lu, "Design verification of large time constant thermal shields for optical reference cavities," Rev. Sci. Instrum. **87**, 023104 (2016).
[32]Ch. Salomon, D. Hils, and J. L. Hall, "Laser stabilization at the millihertz level," J. Opt. Soc. Am. B **5**, 1576 (1988).
[33]T. Day, E. K. Gustafson, and R. L. Byer, "Sub-hertz relative frequency stabilization of two-diode laser-pumped Nd:YAG lasers locked to a Fabry-Perot interferometer," IEEE J. Quantum Electron. **28**, 1106–1117 (1992).
[34]O. Mor and A. Arie, "Perfromance analysis of Drever-Hall laser frequency stabilization using a proportional + integral servo," IEEE J. Quantum Electron. **33**, 532 (1997).
[35]J. Millo, M. Merzougui, S. D. Pace, and W. Chaibi, "High bandwidth frequency lock of a rigid tunable optical cavity," Appl. Opt. **53**, 7761 (2014).
[36]G. J. Dick, "Local oscillator induced instabilities in trapped ion frequency standards," in *Proceedings of Precise Time and Time Interval*, *Redondo Beach, CA* (US Naval Observatory, 1987), Vol. 19, p. 133.
[37]M. Schiemangk, S. Spießberger, A. Wicht, G. Erbert, G. Tränkle, and A. Peters, "Accurate frequency noise measurement of free-running lasers," Appl. Opt. **53**, 7138 (2014).
[38]F. Riehle, "Frequency standards basics and applications" (Wiley-VCH Verlag, 2004). Note that in our paper, the notation of S is for linear power spectral density, corresponding to square-root power spectral density in the reference.